Science and Technology Indonesia
*e*-ISSN:2580-4391 *p*-ISSN:2580-4405
Vol. 10, No. 2, April 2025

Research Paper

# Augmenting Chroma Performance for WLED Employing $Sr_8ZnSc(PO_4)_7:Eu^{2+}$@$SiO_2$ as a Scattering-Enhancing Substance

Pham Hong Cong[1], Nguyen Doan Quoc Anh[2]*

[1]*Faculty of Electrical Engineering Technology, Industrial University of Ho Chi Minh City, Ho Chi Minh City, 70000, Vietnam*
[2]*Faculty of Electrical and Electronics Engineering, Ton Duc Thang University, Ho Chi Minh City, 70000, Vietnam*
***Corresponding author**: nguyendoanquocanh@tdtu.edu.vn

**Abstract**
Featuring the $\beta$-$Ca_3(PO_4)_2$ phosphor system, $Sr_8ZnSc(PO_4)_7:Eu^{2+}$ (SZSPOE) phosphor can be used as an alternative to YAG:$Ce^{3+}$ yellow phosphor for the advancement of the white light-emitting diode (WLED). Its potentials are demonstrated in this paper, including the expected emission power and wavelength based on the previous studies and its impacts on WLED illumination properties employing Mie-theory-based scattering simulation and calculation and MATLAB software. SZSPOE phosphor can display a wide yellow discharge peaking at 511 and 571 nm and a redshift upon the increase in doped $Eu^{2+}$ dosage. A phosphor layer comprised of SZSPOE phosphor, $SiO_2$ particles, and silicone gel is simulated for making a WLED. The WLED performance is observed with varying $SiO_2$ amount. Changes in simulation results of the WLED's lighting properties can be attributed to the scattering within the phosphor layer in response to different $SiO_2$ concentrations. Results demonstrate that increasing $SiO_2$ amount can lead to the better spatial color distribution uniformity and luminous output of the WLED. Meanwhile, the lower color rendering index is observed owing to the insufficient red light power. However, the improvement in color uniformity and luminosity alongside the emission tunability of the SZSPO host, SZSPOE phosphor can be a promising candidate for substituting the original YAG:$Ce^{3+}$ for advanced WLEDs.

**Keywords**
White LED, Lambert-Beer Law, Color Rendering Index, Luminous Efficacy, $Sr_8ZnSc(PO_4)_7:Eu^{2+}$

Received: 12 April 2024, Accepted: 21 January 2025
https://doi.org/10.26554/sti.2025.10.2.467-472

## 1. INTRODUCTION

Significant efforts were made in the past to study white light emitting diode (WLED) devices, academically and industrially. These devices became a huge research subject for having significant proficiency, convenient magnitude, low toxicity, durability, as well as low power demand (Loan et al., 2022; Le Thai et al., 2022). As such, they may eventually supersede traditional lights when it comes universal illumination purposes (Tung et al., 2023). On the other, LED devices can merely yield an insignificant portion of illumination as well as singular chroma under one given period. If the goal is attaining white illumination in solid-status illumination, it is necessary to create a discharge covering the observable spectrum with suitable portions. For the purpose of attaining said result, there are three ways to yield white illumination via LED devices: a merger between three-chroma and a LED chip, YAG:$Ce^{3+}$ sample implemented into a blue chip, and UV OR n-UV chip implemented with blue-red-green phosphor mix (Sena et al., 2024). The three-chroma settings suffer from a drawback as different settings perform distinctively under conduct current, dimness, functioning heat level as well as functioning duration. On the other hand, the regulations applied to chroma reliability would escalate the price (Komine and Nakagawa, 2004; Li et al., 2019; Loo et al., 2011). In the case of the merger between YAG:$Ce^{3+}$ and blue chip, the drawback is significant CCT as well as inferior CRI caused by insufficient red element. While implementing red-green-blue phosphor samples into one UV or n-UV may assist in creating white illumination, the procedure requires significant costs with the lumen proficiency deterioration caused by repeating absorptivity price (Hernandez et al., 2006; Muslu and Arik, 2019). WLED devices containing n-UV chips accompanied by one merger between yellow as well as blue phosphor samples displays desirable attributes: adjustable CCT, significant CRI as well as adjustable chroma coordinates. As such, creating yellow phosphor samples excitable within the n-UV zone would be an essential task (Rakotomalala et al., 2016; Richter et al., 2018).

$\beta$-$Ca_3(PO_4)_2$-type phosphors have gained popularity due to their versatile chemical compositions and tunable emission. Many $Eu^{2+}$-activated phosphors' emission colors may be finely

controlled via cation/anion replacement or the solid solution technique. By using isovalent or aliovalent replacements of $Ca^{2+}$ with different cations, overall emission patterns and characteristics may be altered by changing the site distribution of $Eu^{2+}$. Yet, in the case of $Eu^{2+}$-doped $\beta$-$Ca_3(PO_4)_2$-type compounds, there are opposing perspectives on-site distribution and spectrum assignments in previously published publications. Thus, it is critical to comprehend the foundations of probable $Eu^{2+}$ replacements in the $\beta$-$Ca_3(PO_4)_2$ system (Huang et al., 2020; Tian et al., 2023).

Among investigated $Eu^{2+}$-activated $\beta$-$Ca_3(PO_4)_2$-type phosphors, $Sr_8ZnSc(PO_4)_7$:$Eu^{2+}$ (SZSPOE) phosphor is barely reported. Hence in this paper, the possible $Eu^{2+}$ substitutions, emission bands, and application to produce a WLED model are presented. The phosphor's luminescence is built foundationally based on the previous related studies. The simulation of the phosphor layer comprised of the SZSPOE phosphor and $SiO_2$ is presented with Mie-theory-based software and MATLAB program (Setiawan et al., 2019; Shen et al., 2010; Song et al., 2017). Results show that by varying the $SiO_2$ concentration, the color uniformity and luminosity can be improved with the $SiO_2$@SZSPOE phosphor film, making the SZSPOE phosphor a promising alternative to the original YAG:$Ce^{3+}$ for advanced WLEDs. Besides, the simulation results in this work can be applied for comparison and discussion of further experimental research of this SZSPOE application in the WLED.

## 2. EXPERIMENTAL SECTION

### 2.1 Simulation Method

The SZSPOE samples can be created through the solid-state reactivity. Various constituents were employed, which is shown in Table 1. The constituents were blended then sintered within a lowering aerosphere containing 15% $H_2$ as well as 85% $N_2$ under 1300°C within eight hours accompanied by a pulverizing process to guarantee the completion for reactivity (Sun et al., 2017; Gou et al., 2017). A model of WLED device was built via applying a layer of phosphor compound of translucent silicone substance and phosphor mixture of SZSPOE and $SiO_2$ to cover the n-UV/blue chip. Then the package was fired under 120°C within ten hours. Mie-theory-based software and MATLAB program were applied for monitoring the results of lighting performance with varying $SiO_2$ amount. The LightTools software was also applied for 3D simulation of the WLED package.

**Table 1.** Constituents for SZSPOE

| Constituent | Purity |
|---|---|
| $SrCO_3$ | 99.9% |
| ZnO | 99.99% |
| $Sc_2O_3$ | 99.99% |
| $(NH_4)_2HPO_4$ | 99% |
| $Eu_2O_3$ | 99.99% |

## 3. RESULTS AND DISCUSSION

In previous studies on $\beta$-$Ca_3(PO_4)_2$:$Eu^{2+}$, the obtained absorption band was from 300 nm to 450 and even 500 nm, indicating that the phosphor can be excited by the n-UV and blue chips (Zhao et al., 2022; Zhou et al., 2021). Accordingly, owing to the 4f-5d transfer of $Eu^{2+}$ ion, the phosphor emission under such excitation sources can be obtained from 570 nm to 590 nm, indicating the yellow emission energy. Moreover, the $\beta$-$Ca_3(PO_4)_2$ have been recognized for its high thermostability, making it superior to the original YAG:$Ce^{3+}$ phosphor.

Figure 1 below features the changes of the reduced scattering coefficient in the phosphor layer at different wavelengths and $SiO_2$ amount. The observed modifications seem to follow an inverse process, whereby the scattering coefficients decrease from their maximum values as the wavelength increases. This results in a dispersion of the light produced by the blue chip, which propagates and then transforms into rays at higher wavelengths (Sun et al., 2017; Wang et al., 2011; Rui et al., 2009). Then, when the blue-ray dispersion in the front discharge surge with the blue-ray repeating absorptivity and rear-dispersion decreased, the luminescence will be increased. When $SiO_2$ amount increases, the SZSPOE content must decrease in order to achieve this goal. This can be confirmed with the demonstrated data in Figure 2(a) where the SZSPOE concentration is influenced by $SiO_2$ amount. As can be seen, the content considerably falls as the amount of $SiO_2$ escalates. The synchrotron XRD profiles for the Rietveld refinement of SZSPOE is shown by Figure 2(b).

Based on Uitert's work, it is possible to assess potential crystal locations via the formula (Equation (1)):

$$E = Q\left[1 - \frac{v}{4}^{\frac{1}{v}} 10^{nE_a r/80}\right] \quad (1)$$

where $E$ signifies the location for d-line rim within power applying to rare-earth ion. $Q$ signifies the position within power applying to the lower d-line rim in the case of the individual granule. $V$ signifies the valent status for the trigger. $n$ signifies the anion quantity within $Eu^{2+}$ granular exterior. $r$ signifies the radius for the phosphor base's cation superseded with the $Eu^{2+}$ granule. $E_a$ signifies the electronic relation for the granules forming anions (Wu et al., 2012).

Non-radioactive power shift among the $Eu^{2+}$ granules could manifest through reciprocation or electrical multi-pole interactivity. Reciprocation, the cause of power shift under prohibited shifts, needs one huge intersection among the wave functions for the giver as well as receiver. The critical range applying to reciprocation reaches nearly 5 Å, suggesting that reciprocation is not responsible for the power shift among $Eu^{2+}$ ions. On the other hand, power shift among $Eu^{2+}$ granules resulted from non-radioactive electrical multi-pole interactivity. The interactivity among the $Eu^{2+}$ granules is assessed via the formula (Equation (2)) (Wu et al., 2009):

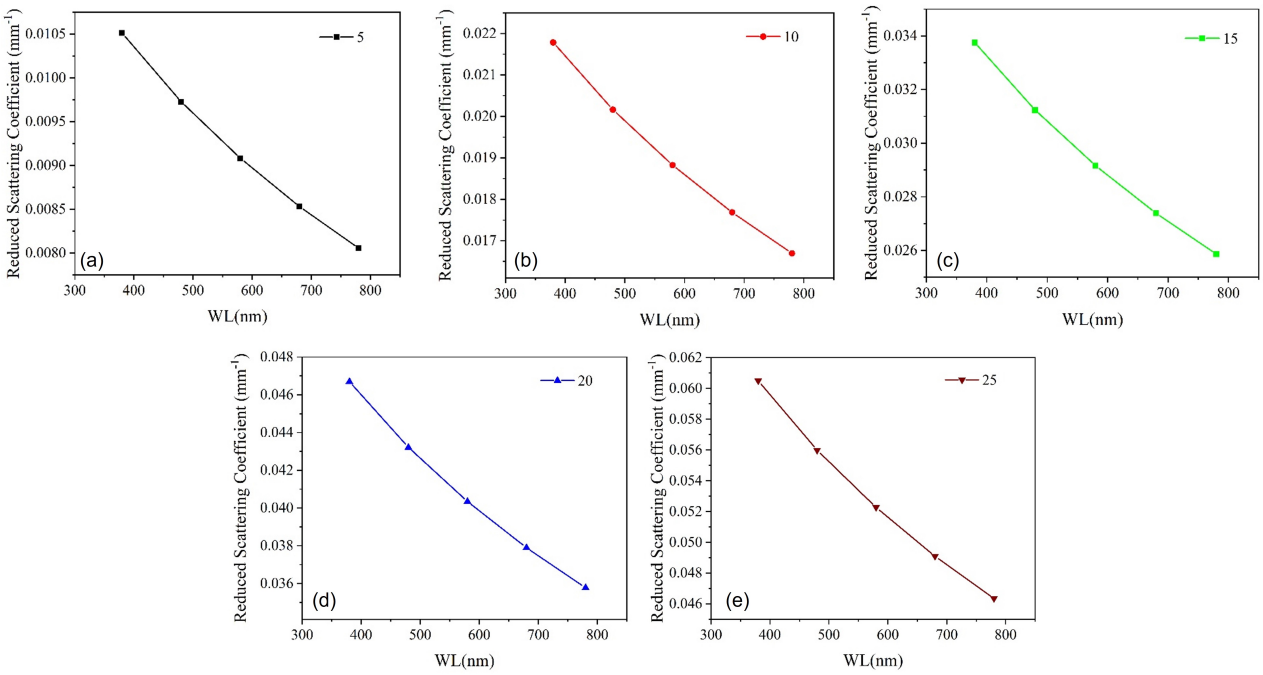


**Figure 1.** Relationship Among Reduced Scattering Coefficient, Wavelength, and $SiO_2$ Amounts: (a) 5%; (b) 10%; (c) 15%; (d) 20%; (e) 25%

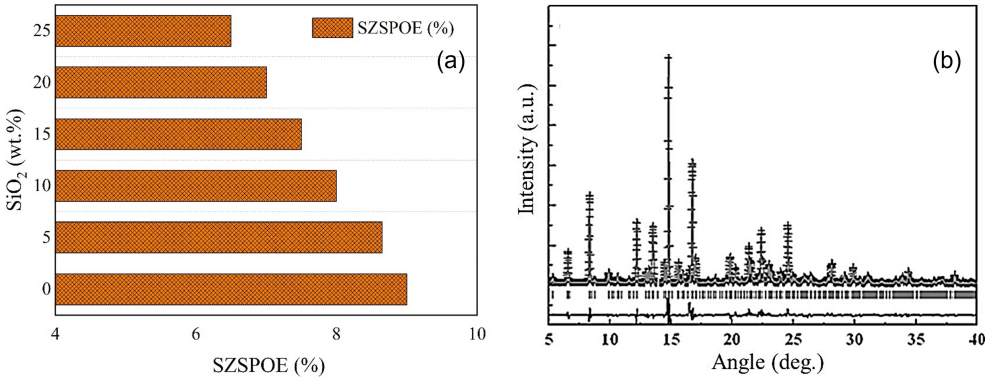


**Figure 2.** (a) Simulated SZSPOE Amount with Different Concentration of $SiO_2$; (b) XRD Profiles for the Rietveld Refinement of SZSPOE

$$\frac{1}{x} = \frac{\kappa}{1+\beta(x)^{\theta/3}} \tag{2}$$

where $\kappa$ and $\beta$ signify the constants applying to an interactivity within one specific phosphor base's latticework. $x$ signifies the trigger dosage. $\theta$ signifies dipole-dipole, dipole-quadrupole, quadrupole-quadrupole interactivities.

The critical range is assessed via Blasse's formula (Equation (3)):

$$R_c \approx 2\left[\frac{3V}{4\pi x_c N}\right]^{1/3} \tag{3}$$

where $V$ signifies cell's capacity. $N$ signifies the phosphor base's cation quantity within a cell.

The amount also affects CCT levels, as shown by Figure 3. The CCT reaches the bottom under 4800 K as *SiO2* amount reaches 25 wt.%. With $SiO_2$ contents are 0 wt.% and 15 wt.%, the CCT surges to the peaks under around 5200 K. The $SiO_2$ concentration has a fluctuating influence on the chroma divergence, as demonstrated via Figure 4. The chroma divergence exhibits irregular declines when the $SiO_2$ content reaches 5 wt.% and beyond. However, under 25 wt.%, the aberration reaches its peak. For the lumen in LED shown in Figure 5, it starts out at its lowest, but shows a consistence rise to the peak as the amount of $SiO_2$ surges.

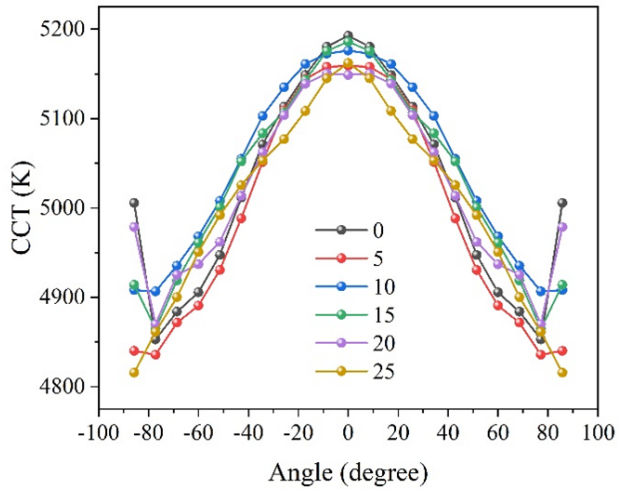


**Figure 3.** Spatial CCT Distribution with Various $SiO_2$ Amount in the Phosphor Layer

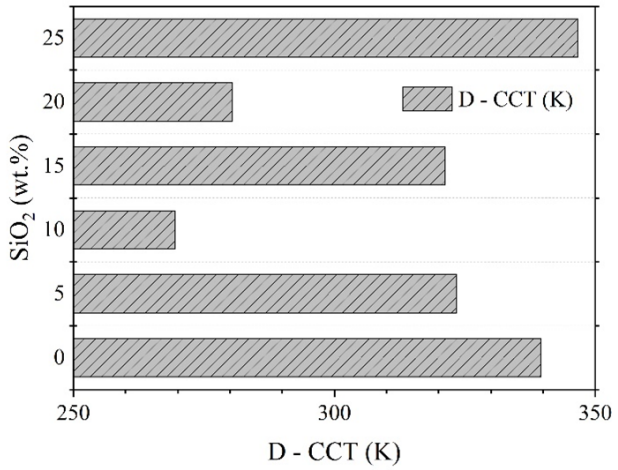


**Figure 4.** Deviated Chroma Level Connected to $SiO_2$ Concentrations

The observed variations may be the consequence of the difference in color allocation and the lower intensity of the blue discharge due to increased rear-dispersion and repeated absorptivity. It should be noted that as the concentration of $SiO_2$ increases, the yellow phosphor concentration has to reduce (see Figure 2), indicating less light absorption events by the phosphor materials. Meanwhile, the scattering by $SiO_2$ is promoted in the phosphor sheet, allowing the incident light to be redirected in the forward ways. As a result, it is possible to enhance the luminosity. Besides, whit proper strength of scattering provided by the $SiO_2$ particles, the combination and distribution of component light spectra are regulated and become more uniform. As a result, the transmuted beam can participate in rear-reflection under extremely large particle sizes, which would enhance the spatial CCT distribution (Zhou and Yan, 2007).

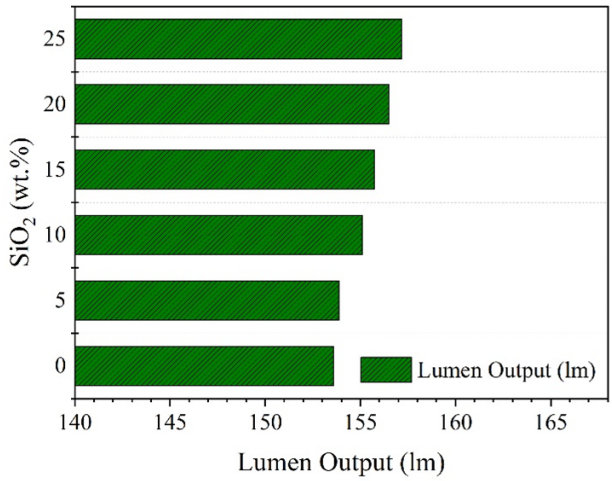


**Figure 5.** LED Lumen Generated Based on $SiO_2$ Amount Variation

The $SiO_2$ amount has an impact on the WLED device's color generation output as well. Figure 6 illustrates a noteworthy decline in CRI that is largely linear as the $SiO_2$ amount grows from 0% to 50%. The color difference involving the orange-yellow, blue, and green components may be the cause of the observed crash. The reason for this discrepancy is that with higher concentration of the scattering particles, the increased dispersion produces more orange-yellow components since the discharge color of the rays often favors the orange-yellow zone. Therefore, excessive dispersion may result in lower CRI and CQS (Zhang et al., 2022).

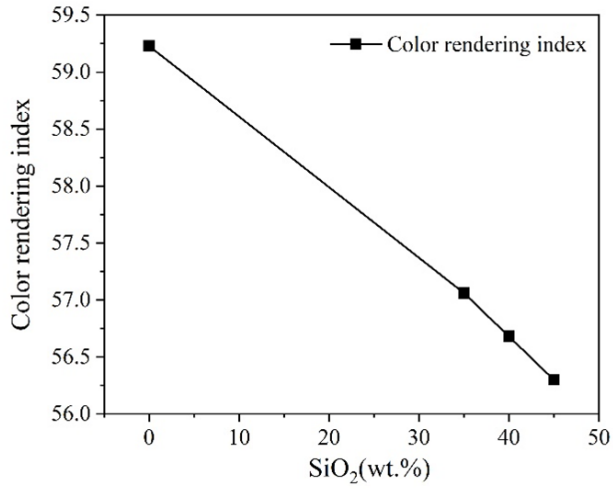


**Figure 6.** CRI Under Influence of $SiO_2$ Amount Variation

Concerning the task of measuring hue quality, CRI would be considered the most common and the oldest index. In order to gauge hue quality, CRI assesses eight hue samples under testing illumination and natural illumination, then compares the conditions. CRI proves to be useful when it comes to assessing

hue performance in illumination with wide spectrum (Zhao et al., 2020). However, this index was developed well before the development of LED devices, and thus, is not suitable to apply on these devices. Using only the few hue samples from CRI, the desaturation resulted would be too much for appropriately assess chromatic output from LED devices. CQS was proposed to remedy this weakness, by assessing fifteen hue samples, and thus is capable of yielding more authentic hue assessments. In addition to increased hue samples, CQS also include other factors: individual's taste and hue disparity. As a newer index proposed in a modern era, CQS would be a more fitting index for examining the hue performance in modern devices like LED (Zhao et al., 2012; Zong et al., 2012). Thus, in the future works, it is essential to include the examination of CQS to evaluate the reproducing color of the light source with proposed photoluminescent materials.

## 4. CONCLUSIONS

This paper demonstrates the potential of SZSPOE phosphor, including its expected emission power and wavelength, based on previous studies and its impacts on WLED illumination properties using Mie-theory-based scattering simulation, calculation, and MATLAB software. The SZSPOE phosphor cam exhibits a broad yellow emission with the peaks located within 570-590 nm, with a redshift as the $Eu^{2+}$ doping concentration increases. A simulated WLED was created using a phosphor layer composed of SZSPOE phosphor, $SiO_2$ particles, and silicone gel. The performance of the WLED was evaluated with varying amounts of $SiO_2$. The changes in the lighting properties of the WLED, as observed in the simulations, are attributed to the scattering effects within the phosphor layer due to different $SiO_2$ concentrations. The results indicate that increasing the $SiO_2$ amount improves the spatial color distribution uniformity and luminous output of the WLED. However, a lower color rendering index was observed due to insufficient red light emission. Despite this, the improvement in color uniformity and luminosity, coupled with the emission tunability of the SZSPO host, suggests that SZSPOE phosphor is a promising candidate for replacing the traditional YAG:$Ce^{3+}$ in advanced WLED applications.

## 5. ACKNOWLEDGMENT

This research is funded by Ton Duc Thang University under grant number FOSTECT.2024.22.

## REFERENCES

Gou, J., J. Fan, M. Luo, S. Zuo, S. Ye, L. Ma, Y. Chen, M. Wang, X. Wang, and B. Yu (2017). $Sr_8ZnSc(PO_4)_7$: $Eu^{3+}$, $Li^+$ Novel Red-Emitting Phosphors: Synthesis and Photoluminescence Properties. *Materials Research Bulletin*, **86**; 234–240

Hernandez, F. L., E. Poves, R. Perez-Jimenez, and J. Rabadan (2006). Low-Cost Diffuse Wireless Optical Communication System Based on White LED. In *2006 IEEE International Symposium on Consumer Electronics*. IEEE, pages 1–4

Huang, X., Z. Qiao, Z. Qiu, N. Ma, J. Wen, and L. Ning (2020). Site Occupation and Spectral Assignment in $Eu^{2+}$-Activated $\beta$-$Ca_3(PO_4)_2$-Type Phosphors: Insights from First-Principles Calculations. *Inorganic Chemistry*, **59**(22); 16760–16768

Komine, T. and M. Nakagawa (2004). Performance Evaluation of Visible-Light Wireless Communication System Using White LED Lightings. In *Proceedings. ISCC 2004. Ninth International Symposium on Computers And Communications (IEEE Cat. No. 04TH8769)*, volume 1. IEEE, pages 258–263

Le Thai, N., T. M. Bui, H. Y. Lee, and N. D. Q. Anh (2022). Phosphor Conversion for WLEDs: YBO3: $Ce^{3+}$, $Tb^{3+}$ and its Effects on the Luminous Intensity and Chromatic Properties of Dual-Layer WLED Model. *Materials Science-Poland*, **40**(4); 105–113

Li, J. X., J. L. Zheng, X. W. Du, Z. T. Li, and J. S. Li (2019). Enhancement of Optical Performance for Quantum Dot White LEDs with Semi-Shperical Lens Packaging Structure using SiO 2 nanoparticles. In *2019 20th International Conference on Electronic Packaging Technology (ICEPT)*. IEEE, pages 1–4

Loan, N. T. P., N. D. Q. Anh, N. C. Trang, and H.-Y. Lee (2022). Better Color Distribution Uniformity and Higher Luminous Intensity for LED by Using a Three-Layered Remote Phosphor Structure. *Materials Science-Poland*, **40**(1); 60–67

Loo, K. H., Y. Lai, and K. T. Chi (2011). A Low-Cost Method for Minimizing the Chromaticity Shift of DC-Driven Phosphor-Converted White LEDs by Thermal Design. In *8th International Conference on Power Electronics-ECCE Asia*. IEEE, pages 515–519

Muslu, A. M. and M. Arik (2019). Impact of Electronics Over Localized Hot Spots in Multi-Chip White LED Light Engines. In *2019 18th IEEE Intersociety Conference on Thermal and Thermomechanical Phenomena in Electronic Systems (ITherm)*. IEEE, pages 31–39

Rakotomalala, L., Z. Randriamanantany, S. Hartopanu, R. Hertanu, and D. D. Lucache (2016). Variance of Radiometric Performances for Cool-White and Neutral-White LED Luminaries. In *2016 International Conference and Exposition on Electrical and Power Engineering (EPE)*. IEEE, pages 520–524

Richter, K., S. Aleksic, and C.-A. Bunge (2018). Estimating the Modulation Characteristics of White Leds by Their Color Temperature. In *2018 20th International Conference on Transparent Optical Networks (ICTON)*. IEEE, pages 1–4

Rui, W., D. Jing Yuan, S. An Cun, W. Yong Jie, and L. Yu Liang (2009). Indoor Optical Wireless Communication System Utilizing White LED Lights. In *2009 15th Asia-Pacific Conference on Communications*. IEEE, pages 617–621

Sena, S., S. Kumari, V. Kumar, and A. Husen (2024). Light Emitting Diode (LED) Lights for the Improvement of Plant

 

Performance and Production: A Comprehensive Review. *Current Research in Biotechnology*, **7**; 100184

Setiawan, E., T. Adiono, I. N. Osahon, and W. O. Popoola (2019). Experimental Demonstration of Visible Light Communication Using White LED, Blue Filter and SoC Based Test-Bed. In *2019 International Symposium on Electronics and Smart Devices (ISESD)*. IEEE, pages 1–4

Shen, C. Y., K. Li, Q. L. Hou, H. J. Feng, and X. Y. Dong (2010). White LED Based on YAG: Ce, Gd Phosphor and CdSe–ZnS Core/Shell Quantum Dots. *IEEE Photonics Technology Letters*, **22**(12); 884–886

Song, J., W. Zhang, L. Zhou, X. Zhou, J. Sun, and C.-X. Wang (2017). A New Light Source of VLC Combining White LEDs and RGB LEDs. In *2017 IEEE/CIC International Conference on Communications in China (ICCC)*. IEEE, pages 1–6

Sun, J., Y. Peng, H. Zheng, X. Guo, Z. Gan, and S. Liu (2017). Enhancing ACU of White LEDs by Phosphor Coating Based on Electrohydrodynamics. *IEEE Photonics Technology Letters*, **29**(4); 393–396

Tian, J., J. Xie, and W. Zhuang (2023). Recent Advances in Multi-Site Luminescent Materials: Design, Identification and Regulation. *Materials*, **16**(6); 2179

Tung, H. T., D. A. N. Thi, and N. D. Q. Anh (2023). The Effects of $Ca_{14}Mg_2(SiO_4)_8$: $Eu^{2+}$ Phosphor on White Light Emission Quality of LED-Phosphor Packages. *Bulletin of Electrical Engineering and Informatics*, **12**(6); 3388–3394

Wang, J., Z. Kang, and N. Zou (2011). Research on Indoor Visible Light Communication System Employing White LED Lightings. In *IET International Conference on Communication Technology and Application (ICCTA 2011)*. IET, pages 934–937

Wu, F., W. Zhao, S. Yang, and C. Zhang (2009). Failure Modes and Failure Analysis of White LEDs. In *2009 9th International Conference on Electronic Measurement & Instruments*. IEEE, pages 4–978

Wu, F.-M., C.-T. Lin, C.-C. Wei, C.-W. Chen, H.-T. Huang, and C.-H. Ho (2012). 1.1-Gb/s White-LED-Based Visible Light Communication Employing Carrier-Less Amplitude and Phase Modulation. *IEEE Photonics Technology Letters*, **24**(19); 1730–1732

Zhang, X., Y. Peng, J. Li, and T. Shi (2022). Opto-Thermal Performances Investigation of Phosphor-in-Glass Based Chip-Scale White LEDs. In *2022 23rd International Conference on Electronic Packaging Technology (ICEPT)*. IEEE, pages 1–4

Zhao, F., G. Dong, G. Yang, Y. Zeng, B. Shieh, and S. R. Lee (2020). Study on Light Emitting Surface Temperature of LEDs. In *2020 21st International Conference on Electronic Packaging Technology (ICEPT)*. IEEE, pages 1–5

Zhao, H., C. Chen, and S. R. Lee (2012). Effects of GaN Blue LED Chip and Phosphor on Optical Performance of White Light LED. In *2012 2nd IEEE CPMT Symposium Japan*. IEEE, pages 1–4

Zhao, J., J. Dong, J. Zhou, and L. Wang (2022). Sr-Substitution-Guided $Eu^{2+}$ Site Engineering of $Ca_9Nd(PO_4)_7$: $Eu^{2+}$ for High-Efficiency White Light-Emitting Diodes. *Optik*, **267**; 169699

Zhou, J., M. Chen, J. Zhang, C. Shi, J. Ding, Y. Zhuang, and Q. Wu (2021). Regulating Photoluminescence Behavior by Neighboring-Cation-Size in $Sr_8CaX(PO_4)_7$: $Eu^{2+}$ (X= Al and Ga) Phosphors for High Color Rendering Solid-State Lighting Source. *Chemical Engineering Journal*, **426**; 131869

Zhou, J. and W. Yan (2007). Experimental Investigation on the Performance Characteristics of White LEDs Used in Illumination Application. In *2007 IEEE Power Electronics Specialists Conference*. IEEE, pages 1436–1440

Zong, S., J. Wu, and X. He (2012). A Novel Method for Illumination and Communication Using White LED Lights. In *6th IET International Conference on Power Electronics, Machines and Drives (PEMD 2012)*. IET, pages 1–5

 